Emulation-Based Robustness Assessment for Automotive Smart-Power ICs

Manuel Harrant
Thomas Nirmaier
Jérôme Kirscher
Infineon Technologies AG
Neubiberg, Germany
Manuel.Harrant@infineon.com

Christoph Grimm
Technische Universität Kaiserslautern
Kaiserslautern, Germany

Georg Pelz
Infineon Technologies AG
Neubiberg, Germany

***Abstract*—In this paper we present a concept for assessing the robustness of automotive smart power ICs through lab measurements with respect to application variance and parameter spread. Classical compliance to the product specification, where only minimum and maximum values are defined, is not enough to assess device robustness since complex transients of application components cannot be defined within single specification parameters. That is why application fitness becomes a necessary task to reduce device failures, which may occur in the application. One solution would be to enhance traditional lab verification methods with a concept that considers application and parameter spread. This innovative concept is demonstrated on an electronic throttle control application. It has been emulated in real-time, including power amplification and application-relevant parameters. Monte Carlo experiments were carried out within the application space to evaluate the influence of parameter spread on selected system characteristics. Finally, an appropriate metric was used to quantify the robustness of the micro-electronic device within its application.**

Keywords: Automotive Power Micro-electronics, Electronic Throttle Control, Post-Silicon Verification, Application Fitness, Worst-Case Distance

I. Introduction

Robustness of automotive smart power micro-electronics can be defined as the ability to operate safe and reliable under all possible operating conditions or, not to fail under any allowed condition. Traditional post-silicon verification tends to check the compliance of device behavior to the product specification. It is obvious that compliance with the specification is a necessary condition, but does not necessarily confirm that the device is working safe and reliable inside its target application since the specification provides no statement about application profiles. A necessary additional task is to assess application fitness and provide a metric for the robustness of the device under test within its application.

Monte Carlo experiments with access to the full application space [1] allow to analyze and evaluate a system characteristic dependent on spread of application parameters. Hence, it is possible to generate large statistics but there is no quantified metric about application fitness of the device under test.

This research project *RESCAR 2.0* is supported by the German Government, Federal Ministry of Education and Research under the grant number 01M3195.
978-3-9815370-2-4/DATE14/©2014 EDAA

Therefore, we want to assess robustness of automotive power micro-electronic devices by using an appropriate metric for single specification parameters when considering variances in their target application [2]. There are different types of metrics which can be used to quantify how a performance parameter is correlated to a corresponding specification border. Examples in this case can be, for instance, the Worst-Case Distance (WCD) [3], [4]. WCD is commonly used for yield analysis and design centering. Furthermore, Response Surface Models [5], [6] are used for minimizing influences of application parameters, such as parameter spread of external components, on system characteristics based on polynomial metamodels.

The paper is organized as follows. In Chapter II, we discuss different concepts for emulation topics and point out limitations compared to the presented approach. The concept for emulating different parts of automotive applications for mixed-signal power devices is presented in Chapter III and demonstrated for an electronic throttle in Chapter IV. An evaluation of the electro-mechanical system is provided in Chapter V while experimental results combined with a statistical analysis is presented in Chapter VI. Chapter VII concludes this paper with a summary and outlook for future work in this research area.

II. Related Work

There is a wide range of research activities related to Hardware-in-the-Loop (HIL) topics since they offer a good solution for testing equipment in a safe way and an early stage during the development process of (micro-) electronic devices. Classical Hardware-in-the-Loop approaches offer a connection between micro-electronic device and target application or environment that is simulated on different types of signal processors, such as DSP, FPGA or power PC.

Meanwhile, these concepts are used in different areas, such as testing the correct functionality of control algorithms [7], [8] (e.g. a simulated motor controlled by a pulse width modulated (PWM) signal) or checking communication and sensor interfaces [9]–[11]. Under these conditions, the system gives feedback about interactions between the device under test and the real-time simulated application as long as they only refer

on digital signal exchange. If the behavior of device under test depends on real power levels (e.g. current flow through a motor bridge dependent on the motor characteristics), these approaches reach their physical limits.

In order to overcome this limitation, a further development of these systems was introduced, called Power Hardware-in-the-Loop (PHIL). Compared to traditional Hardware-in-the-Loop solutions, PHIL systems include power amplification concepts to convert digital values into analog power levels. This enhancement allows the analysis of the device's electrical behavior based on real power levels. Research in this field goes in different directions, such as emulation topics in the area of lithium-ion battery cells [12], [13] or electrical alternators [14], [15]. Although these approaches are emulating different types of voltage sources, they are not applicable for emulation topics in the area of electric drive systems and motor applications.

Emulation topics, which are more related to electric drive systems can be found in the area of motor emulation. There are existing approaches emulating the electric behavior of several types of motors, such as DC motors [16], [17] and multi-phase motors [18], [19]. Limitation of these approaches is often their low bandwidth. Electrical motors for engine management tasks, such as an automotive electronic throttle, are controlled with fast switching PWM signals for an optimal control of airflow inside the internal combustion engine. Since the sample rate of the PHIL system goes hand in hand with the accuracy of the approach, it is necessary to achieve high closed-loop speeds when assessing the robustness of the device under test with respect to the target application.

Beside low bandwidth problems, further challenges that must be solved when emulating these types of complex systems, is the modeling of mechanical behavior and how mechanics influence the electrical behavior of the motor. The electronic throttle control application is an electro-mechanical system, where a DC motor is connected to a mechanical system consisting of gear transmission and throttle valve. For emulation topics and for robustness assessment of this automotive application, it is necessary to have access to both, electrical as well as mechanical parameters.

III. Emulation Concept of an Automotive Throttle

The hardware architecture for emulating motors controlled by any type of integrated motor bridge is a further development of the load emulation concept, which was presented in [20] to emulate incandescent light bulbs or lithium-ion battery cells. For automotive power load emulation topics, the system was configured to act as a controlled current sink connected to the output of a smart high-side switch. For lithium-ion battery cell emulation, the system acts as a controlled voltage source, setting up the cell voltages based on its charge and discharge current. The hardware concept for the presented use case, when emulating an electronic throttle valve connected to any type of integrated motor bridge, is depicted in Figure 1.

The model equations for the electro-mechanical system are evaluated in real-time on the FPGA separately for both load channels $CH2$ and $CH3$. In case of using integrated motor

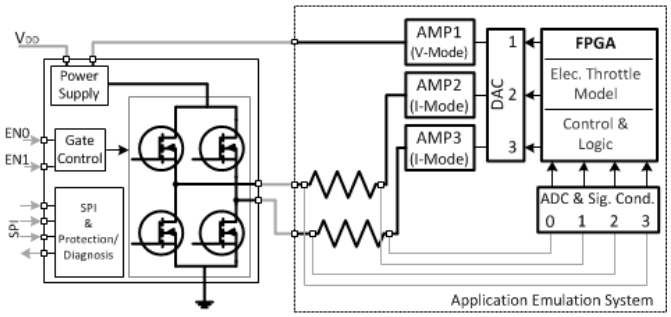

Fig. 1. Hardware setup for emulation of an electronic throttle valve

bridges, the control of the power amplification circuit is more complex compared to the concept used in [20]. In the real application, the electro-mechanical system is located between one low-side/high-side pair of the motor bridge. One side of the motor bridge is triggered with the same digital enable signal while the low-side drivers contain inverters at their gate connection to prevent short circuits between V_S and ground. For an emulation of the DC motor in this configuration, it is necessary to distinguish between two states.

- If the high-side drivers are switched on, the respective amplifier channel must behave as a current sink.
- If the low-side drivers are switched on, the respective amplifier channel must behave as a current source.

The transition between current source and current sink (substituted with *Control & Logic* in Figure 1) is linked to the digital enable signals, which are used to control the integrated motor bridge. This is why the closed-loop frequency of the application emulation system is of great importance to minimize errors coming from the dynamic re-configuration between sinking and sensing current. Furthermore, $CH1$ of the multi channel power amplifier was configured to generate the supply voltage V_S of the device under test. This extension allows an easy and automated adjustment of V_S or, in case of further exploration of the verification space, an evaluation of the battery model including parts of the automotive wiring harness, whose simplified model was already presented in [1].

Beside hardware architecture, software is required to control the application emulation system. The software needs to provide the following tasks for assessing robustness of micro-electronic devices, besides control of the emulation system:

- Automated measurement execution.
- Resolve statistical variations of selected parameters.
- Post-processor for report generation and analysis steps.

The final software implementation to solve the requirements listed above is the extension of an existing lab automation environment, presented in [21]. The software extension for controlling the application emulation system is a graphical user interface, which is remotely configurable on the basis of the existing measurement and automation environment, developed in Labview. This software is able to control external equipment (e.g. oscilloscope, DC power supply) via general purpose interface bus interface and the application emulator

via ethernet connection. An integrated real-time controller, implemented inside the application emulator, handles data transfer, save voltage and corresponding current waveforms in its internal memory and send it instantly to the software running on the host PC. After finishing the test, a report generator, which has access to a subset of Matlab functions, post-processes the raw data coming from the emulator. Based on this report, a routine calculates robustness metrics (e.g. WCD values) for pre-defined device parameters.

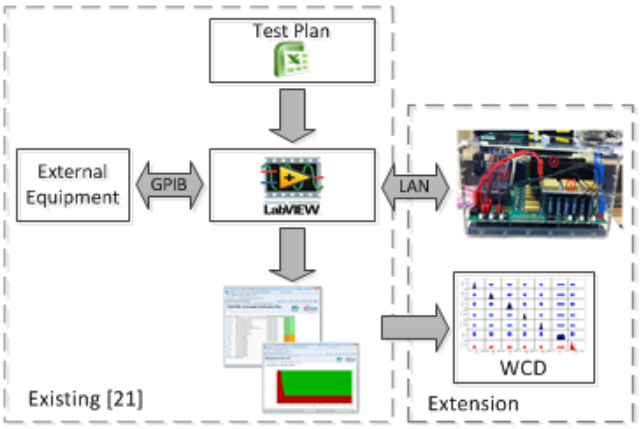

Fig. 2. Software architecture for automotive application emulation

IV. Model of an Electronic Throttle Valve

As an implementation example, the electronic throttle control (ETC) within automotive applications has been chosen. This application, presented in Figure 3, contains electrical components in form of a DC motor as well as mechanical components like gear transmission and a throttle valve. There are models of these electrical and mechanical components available in different languages like Matlab/Simulink, VHDL-AMS, SystemC-AMS, etc. For our approach we present a different modeling flow to evaluate the differential equations of this electro-mechanical system in real-time on a FPGA and control the current flowing through the integrated motor driver with a dynamically configured and controlled power amplifier [20]. Compared to classical mixed-signal simulation models, which are using implicit differential equation solvers, our approach requires the transformation from differential equations to difference equations to be solved by the FPGA.

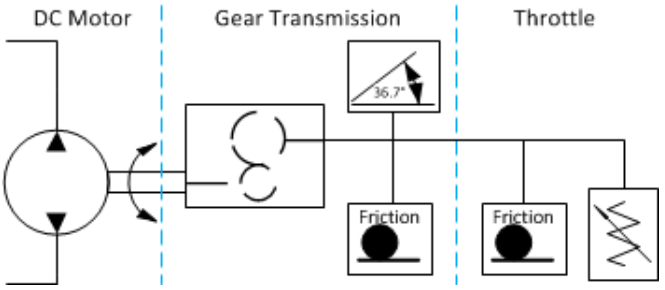

Fig. 3. Components of an automotive electronic throttle

DC Motor:

The model of the DC motor is based on an electro-mechanical model, considering the armature resistance, armature inductance and the back electro-motive force (Back-EMF) for the electrical part and the generated torque and power losses for the mechanical part. This behavioral model and a way for extracting motor parameters was presented in [22] and used for simulation of the advanced front lighting where an electric motor controls the high beam headlight leveling. The following equation expresses the electrical behavior of the DC motor:

$$v_{DUT}(t) = k_t \cdot \omega_{Motor} + R_{Motor} \cdot i(t) + L_{Motor} \cdot \frac{di}{dt} \quad (1)$$

where $v_{DUT}(t)$ is the time-variant voltage at the DUT output, $i(t)$ is the motor current, R_{Motor}, L_{Motor} are the armature resistance and armature inductance, respectively, while k_t is the torque constant. The mechanical behavior of the DC motor is modeled according to the following expression:

$$T_{Motor}(t) = -k_t \cdot i(t) + D_{Motor} \cdot \omega_{Motor} + J_{Motor} \cdot \frac{d\omega_{Motor}}{dt} \quad (2)$$

where T_{Motor} is the generated torque, D_{Motor} is the damping constant and J_{Motor} is the moment of inertia of the DC motor.

Mechanical subsystem:

The mechanical part of the electronic throttle valve application contains a gear connected to some kind of mass-spring system. The gear transmission expresses the following relationships:

$$T_{Gear,out} = g_{Gear} \cdot T_{Motor} \cdot \eta_{Gear} \quad (3)$$

$$\omega_{Gear} = \frac{\omega_{Motor}}{g_{Gear}} \cdot \eta_{Gear} \quad (4)$$

where $T_{Gear,out}$ is the torque dissipated by the complete mechanics, $\omega_{Gear,out}$ is the angular velocity at the gear's output and g_{Gear} is the gear transmission ratio. η_{Gear} represents the degree of effectiveness, which must be added when considering non-ideal components.

Additionally, the gear transmission is also afflicted from power losses like inertia and viscous friction of the mechanics and can be modeled as follows:

$$T_{Gear,Inertia} = J_{Gear} \cdot \frac{d\omega_{Motor}}{dt} \quad (5)$$

$$T_{Gear,Friction} = D_{Gear} \cdot \int d\omega_{Motor} dt \quad (6)$$

where J_{Gear} is the moment of inertia and D_{Gear} is the damping of the gear. This leads to the following torque T_{Mech} that is consumed by the complete mass-spring system replacing the throttle valve:

$$T_{Mech} = T_{Gear,out} - T_{Gear,Inertia} - T_{Gear,Friction} \quad (7)$$

The throttle itself suffers, just as the motor and the gear transmission, from power losses caused by friction and inertia of non-ideal components. The whole torque consumption can be calculated based on Kirchhoff's law for mechanical nodes:

$$T_{Mech} = T_{Th,id} + T_{Th,Loss} \tag{8}$$

where $T_{Th,id}$ is the torque of the ideal mass-spring system and $T_{Th,Loss}$ describes power losses inside the throttle. Replacing both parts of the torque with model parameters of the physical mass-spring system leads to the following expressions:

$$T_{Th,id} = D_{Spring} \cdot (\int \omega_{Gear} dt + \theta_{Init}) \tag{9}$$

$$T_{Th,Loss} = J_{Spring} \cdot \frac{d\omega_{Gear}}{dt} \tag{10}$$

where D_{Spring} stands for the spring constant, J_{Spring} is the inertia of the mechanical subsystem and θ_{Init} defines the initial angle of the throttle valve. In the real application, the throttle valve is not completely closed to prevent freezing in case of low ambient temperature.

The last part of the throttle mechanics is the limiter, which defines the maximum valve opening. Unlike the remaining parts of the whole electro-mechanical system, the limiter has no continuous behavior that can be modeled according to physical equations. For that reason, the limiter was treated as a state transition for the torque consumed by the mechanics:

$$T_{Mech} = \begin{cases} T_{Th,id} + T_{Th,Loss} & \theta < \theta_{Max} \\ k_{Stop} \cdot (\theta_{Max} - \int \omega_{Gear}) + T_{Th,Loss} & \theta \geq \theta_{Max} \end{cases} \tag{11}$$

where k_{Stop} is the damping constant of a non-movable object and θ_{Max} is the maximum valve opening position.

Combining all equations listed in this section leads to a set of three difference equations containing three unknown state variables. Hence, this mathematical system of equations is solvable in the discrete time domain by the FPGA, whose block level model of the DC motor is depicted in Figure 4. All application parameters are connected in variable clusters, which can be modified in an automated way using the automation environment described in Section III.

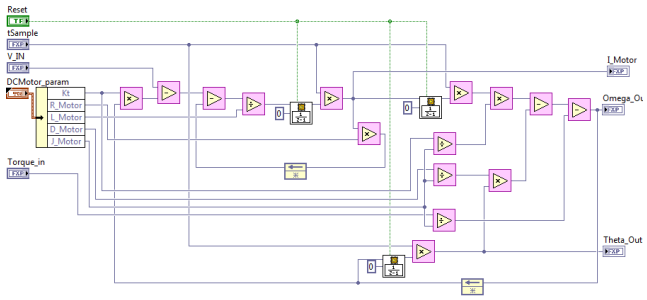

Fig. 4. Model of electronic throttle application in Labview FPGA toolbox

V. Model Evaluation of the Electronic Throttle

First measurements were obtained to evaluate the precision of the electro-mechanical system at different points of the application space. Therefore, system simulation results of the whole application were compared to the emulated throttle connected to the physical motor bridge. In the following, the model accuracy was evaluated based on different test cases, described in Table I:

TABLE I
Test Cases for Model Evaluation

	V_S	R_{Motor}	D_{Valve}
(1) Nominal	$9\ V$	$1.0 \cdot R_{Motor,nom}$	$1.0 \cdot D_{Valve,nom}$
(2) Corner 1	$16\ V$	$0.8 \cdot R_{Motor,nom}$	$0.8 \cdot D_{Valve,nom}$
(3) Corner 2	$12\ V$	$1.2 \cdot R_{Motor,nom}$	$1.2 \cdot D_{Valve,nom}$

The comparison of real-time emulation and simulation test bench for three test cases is visualized in Figure 5.

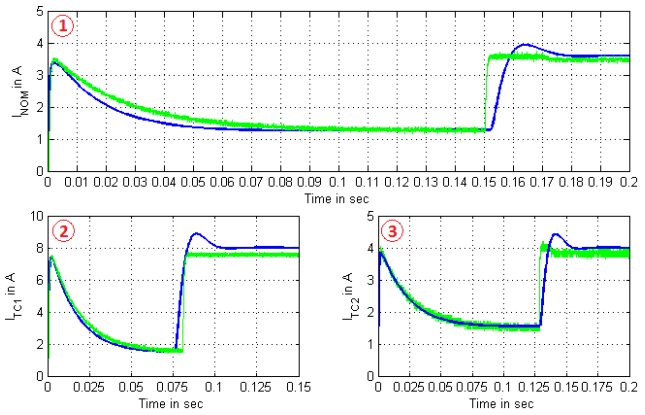

Fig. 5. Comparison of simulation model (blue) and real-time emulated model (green) of an electronic throttle valve

After triggering the device under test, a high inrush current occurred, which decay after a short period of time. The inrush behavior and the maximum value of the current are mainly dependent on the armature resistance and inductance since the back-EMF has no effect when the angular velocity is negligible small. As far as the motor starts rotating, the back-EMF's influence increases leading to a lower current.

In general, neither mixed-signal simulation nor real-time FPGA model contains effects coming from commutation of the motor. Commutation of the motor is necessary to prevent the motor from stopping if the magnetic field of the stator windings goes in the same direction as the magnetic field of the armature windings. This forced reversion of the motor current leads to a periodic discontinuous toggling of the current.

During operation, the emulated behavior of the electro-mechanical system fits with the simulation model with only small deviations during the decreasing phase of the inrush current and the time when the throttle valve reaches its limiter. Remaining errors between simulation and emulation were related to measurement noise, non-ideal system components

(amplifier offset and resolution limitations), fixed-point arithmetic and, last but not least, errors coming from different model implementations. In conclusion, the error between simulation and emulation did not exceed an interval of $\pm$ 5 %.

VI. Experimental Results

For assessing device robustness with respect to the application, the first step is to think about reasonable spread of application parameters. Considering that the model parameters from the characterized electronic throttle are nominal, the main parameters should have a Gaussian distribution coming from manufacturing tolerances, aging effects and parameter spread. Due to the fact that the system must be operational within its full temperature and supply voltage range, operating conditions are uniformly distributed within their maximum operating range. Within the mechanics of the throttle valve, the gear's efficiency η_{Gear} is also uniformly distributed since this parameter cannot be sufficiently characterized. All parameters of the electronic throttle are listed in Table II including their distribution and standard deviation.

TABLE II
Application-relevant parameters of an electronic throttle

Parameter	Description	Distribution	Std. Deviation
(1) DC Motor			
R_{Motor}	Armature resistance	Gaussian	$0.05 \cdot R_{Mot,nom}$
L_{Motor}	Armature inductance	Gaussian	$0.05 \cdot L_{Mot,nom}$
k_t	Torque constant	Gaussian	$0.05 \cdot k_{t,nom}$
D_{Motor}	Motor damping constant	Gaussian	$0.05 \cdot D_{Mot,nom}$
J_{Motor}	Motor moment of inertia	Gaussian	$0.05 \cdot J_{Mot,nom}$
(2) Gear Transmission			
g_{Gear}	Gear transmission ratio	Gaussian	$0.01 \cdot g_{Gear,nom}$
η_{Gear}	Effectiveness of gear	Uniform	0.9...1.0
D_{Gear}	Gear's damping constant	Gaussian	$0.05 \cdot D_{Gear,nom}$
J_{Gear}	Gear moment of inertia	Gaussian	$0.05 \cdot J_{Gear,nom}$
(3) Throttle Valve			
D_{Valve}	Spring constant	Gaussian	$0.05 \cdot D_{Valve,nom}$
J_{Valve}	Valve moment of inertia	Gaussian	$0.05 \cdot J_{Valve,nom}$
θ_{Max}	Position of Limiter	Gaussian	$0.05 \cdot \theta_{Max}$
θ_{Init}	Initial valve opening	Gaussian	$0.05 \cdot \theta_{Init}$
k_{Stop}	Limiter's damping	Gaussian	$0.05 \cdot k_{Stop,nom}$
(4) Operating Condition			
V_S	Supply Voltage	Uniform	6 V...16 V

The main part of application relevant parameters having a Gaussian distribution are performed with a standard deviation $\sigma = 5$ % from its nominal value. This value can be evaluated by characterizing several real throttle valves. Beside supply voltage and the gear's effectiveness, which are uniformly distributed, the gear's transmission ratio has only 1 % standard deviation representing backlash of the gear wheels.

For further experimental results, a subset of tests were additionally simulated to provide a statement about the quality of the robustness metric when calculated out of emulation data. First of all, 2000 Monte Carlo experiments within the full application space were carried out. All parameters listed in Table II were performed within their specified distributions including performance ranges or standard deviation. A subset of these experiments is visualized in Figure 6.

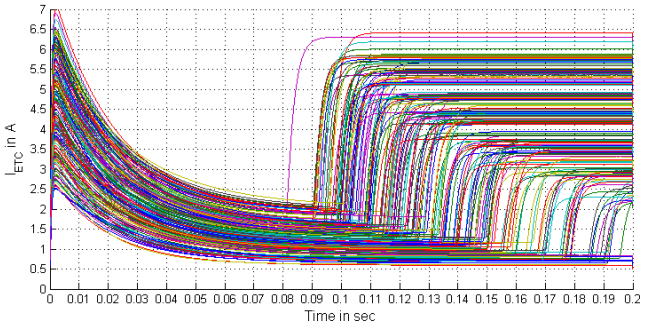

Fig. 6. Current waveforms of 150 selected Monte Carlo experiments with different distributions of throttle parameters and operating conditions

It is obvious that application variances lead to a significant change in the current consumption of the electronic throttle and to the duration until the throttle valve reaches its limiter. The generated torque goes hand in hand with the angular velocity. Such a behavior must be detected by position sensors and control functions within the electronic control unit.

From the electrical point of view, the maximum inrush current I_{MAX} with respect to its specification border is of interest. Smart bridges have current limitations where the high-side driver of the device turns off automatically for a certain period of time to avoid its thermal destruction. This specification parameter $I_{MAX}(L)$ defines the border for safely operating conditions and, in combination with the maximum inrush current, represents a proper scenario for measuring robustness of the device under test. Providing a better overview to the influence of parameter spread and variances coming from the application, Figure 7 shows the matrix plot containing application parameters, which influence the output of interest.

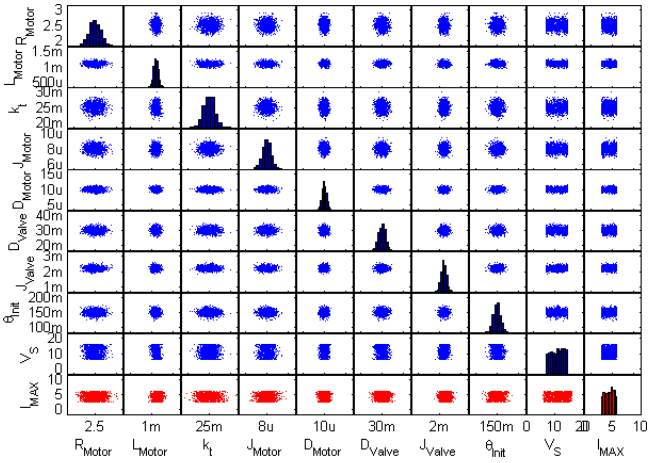

Fig. 7. Matrix plot for the maximum inrush current of an electronic throttle

Basically, matrix plots show dependencies between input parameters and the system response (in the red field) as well as interactions between different input parameters (blue fields). Due to the fact that these plots can visualize data only in two

dimensions, influences coming from other input parameters or measurement noise are visualized as clouds. Interactions, either linear or quadratic, are defined by the trend of the cloud.

The main axis shows the distributions of the throttle parameters and the system response. Based on this distribution and further analyzing steps, different information can be extracted out of the provided data. We were using the Worst-Case Distance (WCD) to get a relationship between application variances and the specification border. The WCD [3], [4] value is defined as the smallest distance between mean of the performance parameter (histogram) and closest specification border multiplied with the standard deviation σ.

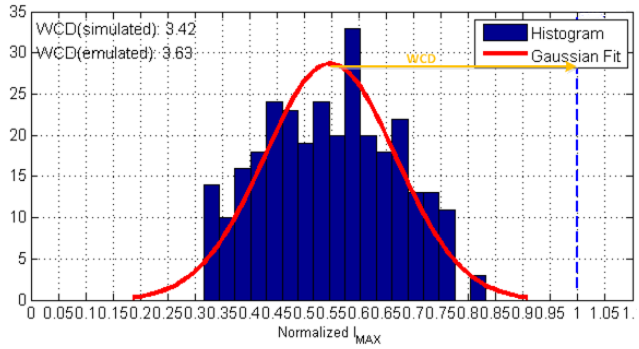

Fig. 8. Evaluation of WCD for the electronic throttle application

Figure 8 shows the response distribution in form of a histogram and its Gaussian fit (red) normalized with the specification border (blue dotted line). Results, which can be finally extracted from this metric are, that the system is not compliant with classical six sigma processes.

VII. Conclusion and Outlook

In this paper we present a concept, which is already productively in use, to measure robustness of automotive smart power devices with respect to application variances during post-silicon verification. Monte Carlo experiments in combination with a statistical analysis have been accomplished based on an electronic throttle valve within automotive vehicles. Experimental results have shown that it is possible to measure robustness metrics out of emulated measurement data to a specification border of a system characteristic. This approach allows verifying automotive smart power products in a way, which is not possible when using real application components.

Future investigations to improve this concept can be the link to a certain mission profile instead of only measuring the robustness to specification borders. The mission profile specifies stress of a system characteristic (e.g. temperature profiles) and generates another border that might be different from the specification boundary.

References

[1] M. Harrant, T. Nirmaier, J. Kirscher, C. Grimm, G. Pelz
Monte Carlo Based Post-Silicon Verification considering automotive application variances, Ph.D. Research in Microelectronics and Electronics (PRIME) 2013, pp. 165-168

[2] T. Nirmaier, J. Kirscher, Z. Maksut, M. Harrant, M. Rafaila, G. Pelz
Robustness Metric for Automotive Power Microelectronics, Design, Automation and Test in Europe (DATE) RIIF Workshop 2013

[3] K. Antreich, H. Graeb, C. Wieser
Practical methods for worst-case and yield analysis of analog integrated circuits, Int.Journal of High Speed Electronics and Systems 1993

[4] K. Antreich, H. Graeb
Circuit optimization driven by worst case distance, IEEE Int. Conference on Computer Aided Design (ICCAD) 1991, pp. 166-169

[5] A. Oros, M. Rafaila, M. Topa, M. Neag, G. Pelz
Application-Oriented Robustness Optimization based on Metamodels, 18th Int. Symposium for Design and Technology in Electronic Packaging (SIITME) 2012, pp. 37-41

[6] M. Rafaila
Planning Experiments for the Validation of Electronic Control Units, Doctoral Thesis, Faculty of Electrical Engineering, Vienna, 2010

[7] Y.H. Hung, C.H. Wu, P.Y. Chen
Development of a Hardware-in-the-Loop Platform for Plug-In Hybrid Electric Vehicles, Int. Symposium on Computer Communication, Control and Automation 2010, pp. 45-48

[8] Y. Lee, W.S. Lee
Hardware-in-the-Loop Simulation of Electro-mechanical Brake, Int. Joint Conference SICE-ICASE 2006, pp. 1513-1516

[9] A.B. Ramirez, D. Rodriguez
Automated Hardware-in-the-Loop Modeling and Simulation in Active Sensor Imaging Using T16713 DSP Units, IEEE Int. Midwest Symposium on Circuits and Systems 2006, pp. 300-304

[10] L. Cheng, Z. Lipeng
Hardware-in-the-Loop Simulation and Its Application in Electric Vehicle Development, IEEE Vehicle Power and Propulsion Conference 2008

[11] H. Zhong, G. Ao, B. Zhou
The Development of a Real-Time Hardware-in-the-Loop Test Bench for Hybrid Electric Vehicles Based on Multi-Thread Technology, IEEE Int. Conference on Vehicular Electronics and Safety 2006, pp. 470-475

[12] L. Gauchia, J. Sanz
A Per Unit Hardware-in-the-Loop Simulation of a Fuel Cell Battery Hybrid Energy System, IEEE Transactions on Industrial Electronics 2010

[13] O. Koenig, C. Hametner, G. Prochart, S. Jakubek
Battery Emulation for Power-HIL Using Local Model Networks and Robust Impedance Control, Transactions on Industrial Electronics 2013

[14] A. Griffo, D. Drury
Hardware-in-the-Loop Emulation of Synchronous Generators for Aircraft Power Systems Electrical Systems for Aircraft, Railway and Ship Propulsion (ESARS) 2012, pp. 1-6

[15] R. Todd, A.J. Forsyth
HIL Emulation of All-Electric UAV Power Systems, IEEE Energy Conversion Congress and Exposition (ECCE) 2009, pp. 411-416

[16] T. Schuster, K. Krischan, G. Dannerer
Emulator for a DC-Machine, working as an actuator in a torque split unit of all-wheel driven automobile, European Conference on Power Electronics and Applications 2007, pp. 1-10

[17] O. Vodyakho, F. Fleming, M. Steurer, C. Edrington
Implementation of a Virtual Induction Machine Test Bed Utilizing the Power Hardware-in-the-Loop Concept, IEEE Electric Ship Technologies Symposium (ESTS) 2011, pp. 52-55

[18] Y.S. Rao, M. Chandorkar
Electrical Load Emulation Using Power Electronic Converters, IEEE Region 10 Conference 2008, pp. 1-6

[19] Y.S. Rao, M. Chandorkar
Rapid Prototyping Tool for Electrical Load Emulation using Power Electronic Converters, IEEE Symposium on Industrial Electronics and Applications (ISIEA) 2009, pp. 106-111

[20] M. Harrant, T. Nirmaier, F. Dona, G. Pelz, C. Grimm
Configurable Load Emulation Using FPGA and Power Amplifiers for Automotive Power ICs, Forum on Specification and Design Languages (FDL) 2012, pp. 84-89

[21] M. Kunze, A. Pirker-Fruhauf
A novel methodology to combine and speed-up the verification process of simulation and measurement of integrated circuits, AUTOTESTCON 2008, pp. 259-262

[22] J. Kirscher, M. Lenz, D. Metzner, G. Pelz
Verification of an Automotive Headlight Leveling Circuit and Application Using Smart Component Property Extraction, IEEE Int. Behavioral Modeling and Simulation Workshop (BMAS) 2008, pp. 1-6